Modeling Turboshaft Engines for the Revolutionary Vertical Lift Technology Project, Expanded

Jeffryes W. Chapman
Aerospace Engineer
NASA Glenn Research Center
Cleveland, Ohio, USA

J. Michael Vegh
Gerardo Nunez
U.S Army DEVCOM
Aviation & Missile Center
Moffett Field, California, USA

Christopher A. Snyder
(Retired) Aerospace Engineer
NASA Glenn Research Center
Cleveland, Ohio, USA

ABSTRACT

Turboshaft engine performance and weight models were developed to support conceptual propulsion and vehicle mission design and performance under the Revolutionary Vertical Lift Technology (RVLT) Project in 2019 by Snyder in Reference 7. These models were developed using open data sources, assuming present and future technology levels, and range from 650 to 5,000 output shaft horsepower (485 to 3,730 kW). This paper expands on the previous research, extending the power ranges from 200 to 15000 output shaft horsepower (150 to 11,200 kW) and documenting the methodology, assumptions, and engine performance realizes important benefits for NASA and the aviation community. NASA concept-vehicle study efforts using these baseline propulsion models can be more readily shared among the government, industry, and university community to support present and future work. Assessing the benefits of advanced technologies and new configurations can be facilitated using these models, which helps guide technology investment. As the various conceptual vehicle and mission analysis simulations are developed, these models can be used directly for broader systems analysis studies, including optimization within the propulsion model itself. To expand on the previous effort, the turboshaft engine is briefly discussed, highlighting the specific components, and expected performance characteristics over the updated power range and technology levels considered. Additional engine configurations will also be discussed as they vary based on power output and assumed technology level. Engine performance, such as airflow, power output and weight are updated, noting important trends for system studies. Finally, the effect of advanced propulsion technologies on public reference models including RVLT concept vehicles are reported along with the tools and software methods used to complete the analysis.

NOMENCLATURE

CFit3	Parametric engine curve fitting tool
CRP	Contingency rated power
DGW	Design gross weight
IC	Intermittent combustion
ISA	International standard atmosphere
IRP	Intermediate rated power
FATE	Future affordable turbine engine
LCTR	Large civil tiltrotor
M	Mach Number
MCP	Maximum continuous power
MRP	Maximum rated power
N_r	Engine rotational speed
NDARC	NASA Design and Analysis of Rotorcraft
NPSS	Numerical Propulsion System Simulation
OPR	Overall pressure ratio
PSFC	Power specific fuel consumption
PT	Power turbine
RPTEM	Referred parameter turboshaft engine model
RVLT	Revolutionary Vertical Lift Technology
SLS	Sea level static
SOA	State of the art
Sp_a	Engine specific power (power normalized by mass flow)
T3	Compression system exit temperature
T4	Turbine inlet temperature
UAM	Urban air mobility
VTOL	Vertical takeoff and landing
WATE++	Weight Analysis of Turbine Engines
$\dot{m}$	Mass flow
η_d	Inlet ram recovery efficiency
γ	Specific heat ratio
θ	Absolute temperature normalized by SLS conditions
δ	Absolute pressure normalized by SLS conditions
θ_M	Inlet ram air temperature ratio
δ_M	Inlet ram air pressure ratio

INTRODUCTION

NASA's Revolutionary Vertical Lift Technology (RVLT) project continues to research and develop technologies to support vertical takeoff and landing (VTOL) vehicles. In 2018, the RVLT project released a set of vehicle / mission models in References 1 and 2 that are representative of the broad variety of vehicles being proposed to fulfill an exciting vision of future urban air mobility (UAM). Care was taken to develop vehicles and missions that could be used to identify and prioritize research and development efforts within the project, but not intentionally endorse or denounce any vehicles or concepts under development. VTOL operations puts unique requirements on propulsion and power systems; therefore, models to better define and understand these systems are important considerations in overall vehicle and mission assessment. Although many UAM concepts are conceived as all-battery electric, present shortfalls in battery energy density and electrical infrastructure suggest that turbine-based generator systems may be advantageous to meet near-term energy needs, enhance vehicle capability, or add operational flexibility.

In this paper, thermodynamic and weight models were developed for the 200 to 15,000 shaft output horsepower (150 to 11,200 kW) range, representative of today's operational and future planned engines. The models were developed using only open sources to allow the models to be freely discussed and distributed. They are parametric in nature to allow the designer to vary engine design parameters for technology assessment and optimization studies; a parallel NASA engine modeling effort is discussed in Reference 3. These engine models are developed within the Numerical Propulsion System Simulator (NPSS, References 4 and 5) software. Once completed they are converted into Referred Parameter Turboshaft Engine Models (RPTEM) using an Army-developed curve fitting toolbox (CFit3). These RPTEM models may be input into the NASA Design and Analysis of Rotorcraft (NDARC, Reference 6) software for the sizing of the concept vehicles. The work show in this paper is an expansion of the work done by Snyder and documented in Reference 7.

Turboshaft engine thermodynamic modeling is discussed first, including methods used, component performance and engine configurations. Engine weight modeling is discussed next, including important factors for the overall design and weight performance. Then overall turbine engine results are discussed, noting how weight and efficiency vary with size and technology level. Details on the software tool chain including a methods discussion of CFit3 with some details of the RPTEM are discussed next. Results from the engine thermodynamic and weight modeling are used for some reference cases (RVLT side by side and tiltwing concept vehicles as well as tandem helicopter and large civil tiltrotor reference models), to show their effect on overall vehicle size and performance.

ENGINE THERMODYNAMIC MODELING

The Brayton thermodynamic cycle is used for engine modeling; the block diagram for a simple, single-spool (core) turboshaft with free power turbine (PT) is given in Figure 1. A free power turbine indicates it is on its own spool (or shaft) and is free to turn at its own rpm. For the rotorcraft application, configuring the PT on its own shaft enables stopping the PT and mechanically connected components (such as vehicle rotors, etc.) without using a clutch mechanism. (This does not preclude the use of an overrunning clutch that allows the rotors to continue rotating freely if the engine stops.) Major engine parameters include overall pressure ratio (OPR) of the engine, compressor pressure ratio (which determines compression system exit temperature, T3), combustor exit temperature (T4), as well as turbomachinery (compressor and turbine) efficiency. A nozzle pressure ratio of 1.1 (nozzle entrance / ambient total pressure) is assumed to set the maximum work from the core gas stream and still leave sufficient gas pressure to exhaust from the engine. A more complete discussion about the Brayton cycle and gas turbines can be found in textbooks such as References 8 and 9. The object-oriented analysis framework, NPSS is used to perform the gas turbine analyses. NPSS contains standard 0/1-D elements for the gas turbine components. These are configured into a representative steady-state, thermodynamic model. Assumptions concerning component performance and specific engine configurations are covered below.

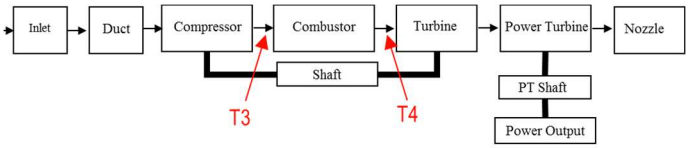

Figure 1. Simple, single-spool turboshaft with free power turbine.

Presented at the Vertical Flight Society's 79th Annual Forum & Technology Display, West Palm Beach, FL, USA, May 16-18, 2023.

Turbomachinery efficiency and flow

Turbomachinery system efficiency and flow are critical factors in gas turbine performance. For this study, turbomachinery polytropic efficiency trends are shown in Figure 2. A discussion of their origin and related information is given in Reference 10. Models for current engines use the current technology line while advanced engines use the advanced technology line. The future trend line is not used in study but is included for completeness. As implemented, technology levels along a particular level or a given fraction between the different technology levels can be set according to configuration. Note: for engine modeling, turbomachinery efficiency is set by the lowest corrected flow rate (core size) found in a specific component; this is based on exit conditions for each compressor component and entrance for each turbine component. Compressor performance maps for flow, speed, efficiency, and stall margin were generated from the computer program reported in Reference 11, based on approximate compressor pressure ratio, compressor type, and expected variable geometries. For turbine performance, performance maps from previous, similar turboshaft engine models are used. All turbomachinery maps are then scaled within NPSS at the engine design point.

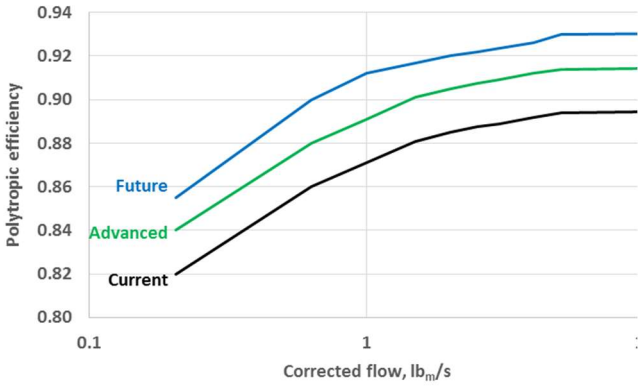

Figure 2. Turbomachinery polytropic efficiency characteristics.

Combustor performance

A simple combustor model is used for all engines, although combustion efficiency and total pressure loss could vary with engine size and technology level. A typical hydrocarbon fuel ($C_1H_{1.94}$) with a lower heating value of 18,400 BTU/lb. (42.8 MJ/kg) and 99.9% combustion efficiency is used. A constant 5% total pressure loss is assumed across the combustor. No combustor cooling airflow is assumed, which for these simple models would be represented as a reduced turbine inlet temperature. These models use NPSS's default gas thermodynamic modeling package, which provides fast and accurate operation for typical kerosene jet fuels. The models can use the more sophisticated gas thermodynamic packages available within NPSS to readily model fuel using any combination of carbon, hydrogen, oxygen, and nitrogen (including hydrogen, sustainable aircraft fuels, and liquid natural gas). This additional flexibility requires only minor user input revisions, mainly the relative amounts of those elements in the fuel and the fuel's lower heating value. Emissions for oxides of nitrogen are not considered in this effort, although it would be simple to add to the models, as was reported in Reference 10.

Turbine cooling

Turbine cooling is another important factor in engine performance. High temperature material choices, engine operational temperatures, and physical blade size all contribute to how much cooling flow can be used and factor into engine weight. The methods discussed by Gauntner in Reference 12 are used to estimate cooling airflow rates. As technology advances, less cooling airflow would theoretically be needed (all other factors being constant). However, more advanced engines tend to have higher OPR, resulting in higher temperature cooling flow and smaller corrected flows in the high-pressure turbine section where the bulk of turbine cooling airflow is used. At smaller corrected flow rates, the turbine material surface area per flow increases – suggesting that cooling airflow would increase as a fraction of turbine airflow. Without definitive information to vary turbine cooling flowrate factors, they are maintained across the various engine models (except as specifically noted later). Turbine cooling parameters can easily be updated to model the effects of higher temperature-capable turbine materials, thermal barrier coatings or more effective cooling technologies.

ENGINE CONFIGURATIONS

Engine configuration includes a variety of factors: number of spools (shafts), whether turbomachinery components use axial or centrifugal / radial flow; and for multiple spools for the core, the split of compression work done on the compressors on each spool. Engine configurations are delineated into 5 sections based on engine power class at maximum rated power at sea level static (MRP, SLS) assuming international standard atmosphere (ISA).

Very small: 250 or less hp class

For this smallest power class, a small number of available (or under development) Brayton engines compete with more numerous options among intermittent combustion (IC), piston engines. Brayton engines are generally smaller and lighter for a given power output and operate with less

vibration than the IC alternatives but cost more in initial engine price and operating fuel use. New materials and manufacturing techniques, along with adding recuperation to Brayton cycles are being explored for advanced cycles to counteract these price and fuel penalties. Recuperation also enables the engine cycle to improve fuel efficiency at lower overall pressure ratios, which reduces turbomachinery cost and complexity (albeit with the recuperator component). Adding recuperation does, however, increase the system weight significantly, which reduces or potentially eliminates the specific power advantage the gas turbine has over IC engines. Current turboshaft engines at this small size would generally be a single-spool design; like the engine noted in Figure 1, but without the free-power turbine. Such simplicity would require a clutch to disengage the engine to allow it to keep spinning while allowing for a stopped rotor. Thus, for RVLT usage, the very small class models assume the single-spool core with the free-power turbine. Turbomachinery is defined as a single stage each for the centrifugal compressor, axial turbine, and axial power turbine. Cooling flow through these engines is very simple and comprised of non-chargeable cooling on the stator. Due to the small size of the turbine blades, cooling channels within the blades may not be possible and blade film cooling isn't an option, so it is assumed there is no chargeable cooling flow. Temperatures near the power turbine are quite low in these engines, so there is no cooling flow in that region. These assumptions are made possible with advanced materials and reduced design operating temperatures.

Small: 400-650 hp class

For this relatively small power class, engine simplicity and therefore cost are again important. These engines are represented by the block diagram shown in Figure 1. Looking at some of the older engines in this power class, the compressor tended to be an axial-centrifugal design to achieve desired engine OPR and efficiency. Reference 13 discusses centrifugal compressor research performed under the small gas turbine engine technology program to enable current single centrifugal stage designs. These single centrifugal stages can achieve the pressure ratio of older, axial-centrifugal at reasonable efficiency levels. The engine configuration then becomes a single centrifugal stage combined with a combustor and a single, axial stage each for the core turbine and the free power turbine. To further reduce weight, titanium instead of steel can be used for the centrifugal compressor and other components. For the advanced version, achieving significantly higher compressor pressure ratio (and therefore potentially higher fuel efficiency) would be difficult within the single centrifugal stage and adding axial stages would compromise simplicity. There are additional considerations going from centrifugal to axial-centrifugal on the same shaft, but that will not be discussed here. The advanced version only includes a slight improvement in turbomachinery efficiency (from current to advanced technology) and minor updates in turbine materials to further reduce weight.

Mid: 1,300 to 3,000 hp class

For the mid power class, additional complexity is warranted for the accompanying improvement in fuel efficiency. References 14 and 15 give engine configuration and performance for the T700 engine, which is used to develop the current technology engine at 2,000 hp. Like the small power class, its configuration is represented by the block diagram in Figure 1. However, the actual compressor design is axial-centrifugal with OPR≈18. For the engine model, the axial and centrifugal portions are modeled separately. The core turbine and free power turbine are both two stages to meet expected efficiency levels. The advanced engine is representative of potential products from the Advanced Affordable Turbine Engine (AATE) demonstrator program; overall goals are found in Reference 16. The advanced engine could be single spool or two spool for its core. References 17 and 18 are white papers from competing company sites discussing the various reasons for choosing either configuration. A configuration like the T901, developed by General Electric, was chosen because the Improved Turbine Engine Program awarded General Electric Aviation to further develop the concept. Turbomachinery efficiency levels were chosen at the advanced level, with some minor additional pressure ratio assumed for both the axial and centrifugal portions of the compressor versus the current engine and an additional free power turbine stage to maintain efficiency at such high energy extraction per airflow.

Large: 5,000 to 7,500 hp class

The large power class includes similar engine configurations as the mid-power class represented in Figure 1, although the compressor for some engines is all axial. One example of an all-axial engine is the Rolls-Royce T406, used for the V-22; similarly, axial-centrifugal designs can also be found. The current engine is modeled using an axial-centrifugal compression and is assumed to be similar to the T55. Engine characteristics for modeling are from References 14 and 19. Current technology levels for turbomachinery efficiency are assumed; T4 and turbine cooling airflow are varied to match stated airflow, power and fuel consumption levels. Reference 16 also discusses the Army's Future Affordable Turbine Engine (FATE) program, which supports advanced engine demonstrators in this class and is used to set performance goals for the advanced engine. A notional version of the GE38/T408 (mid technology engine between many current engines and FATE goals in fuel efficiency) was also modeled. Various

characteristics were compiled from References 14, 20, and 21. Reference 20 is an engine brochure for the T408; which relates its performance to improvements versus the T64. Reference 21 is an engine brochure for the T64. Advanced technology levels for turbomachinery efficiency are assumed, varying OPR and T4 to match compiled characteristics for the T408.

The advanced engine was assumed to meet the FATE engine improvement goals, using the T55 as the baseline configuration. The assumed engine configuration is shown in Figure 3. A two-spool core is assumed to enable the higher engine OPR to meet fuel efficiency targets. Reference 22 discusses some of the reasons for choosing a two- spool core engine configuration. Advanced technology is assumed for turbomachinery efficiency, with compression work split 30% on the low spool and 70% on the high spool, as discussed in References 10. Splitting the compression work between two spools not only enables higher engine OPR but also can reduce the number of turbomachinery stages in the core. The low-pressure spool compressor is assumed all axial, while the high spool is axial-centrifugal. The engine is sized at 7,500 horsepower output.

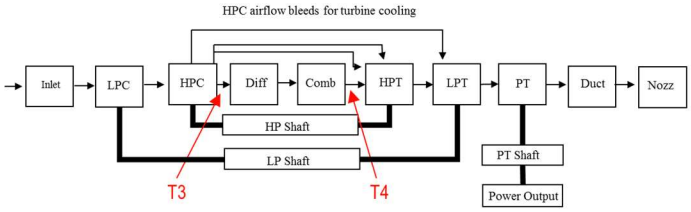

LPC – low pressure compressor, HPC – high pressure compressor, Diff – diffuser, Comb – Combustor, HPT – high pressure turbine, LPT – low pressure turbine, PT – power turbine, Nozz – nozzle, HP – high pressure, LP – low pressure, PT – Power turbine,

Figure 3. Three-spool (two-spool core) turboshaft with free power turbine.

Very large: 11,000 to 15,000 hp class

The very large engine class increases the power significantly from the large power class. Examples of this size of engine include the TP400 turboprop that produces 11,500 horsepower as discussed in Reference 14. Configurations at this size follow the design shown in Figure 3. The increase in airflow prompts a two-spool core and all axial compressors and turbines that drive a free power turbine. The state-of-the-art (SOA) turboshaft was modeled after the TP400 with pressure ratios taken from public sources. Operating temperatures assumed for SOA material choices, with cooled core turbines and an uncooled power turbine. The OPR of this turboshaft is slightly less than that of the FATE configuration due to limits in core size with the all-axial configuration.

The advanced engine produces 15,000 horsepower and uses the SOA as a baseline. Advanced technology includes higher efficiency turbomachinery and the high temperature materials assumed for the large engine class. This results in a combination of higher operating temperatures and a reduction in cooling flow. These advanced technologies reduce the engine core size, however OPR remains the same as the SOA version due to advances in compressor efficiency at low core size.

ENGINE FLOWPATH AND WEIGHT ESTIMATION

Following the engine thermodynamic model development, engine weights and flow path dimensions are developed. The NASA software tool, WATE++ (Weight Analysis of Turbine Engines, Reference 23), is used to create engine architectures that could achieve the engine thermodynamic cycles produced by the NPSS models detailed in the previous sections. The cycle data required for WATE++ execution, such as air mass flow, temperatures, pressures, pressure ratios, etc., are derived from the engine thermodynamic model output. Both the engine design point (maximum rated power, sea level static) and off-design cases are used to encompass the maximum performance level (i.e., temperature and pressure) required to size each engine component. The cycle data, the material properties, and design rules for geometric, stress, and turbomachinery stage-loading limits are used to determine an acceptable engine flow path. Representative engine flow paths for each of the engine configuration are shown in Figure 4.

Stainless steel is used for the compressor components for current technology engines, except the very small and small class engines. For the advanced engines, a titanium alloy is used to significantly reduce compressor and overall engine weight. The small and very small class engine materials are modeled after the Arrius 2B1 engine that is found in Reference 14. Titanium is used for the current engine instead of stainless steel to reflect the current material trend in small turboshaft engines; Arrius 2B1 has a titanium compressor. Nickel-based alloys with specialized heat treatments are used for the turbine components for all the engines. The nickel-based alloys have a higher density and are heavier but are required to withstand the high-temperature turbine environment.

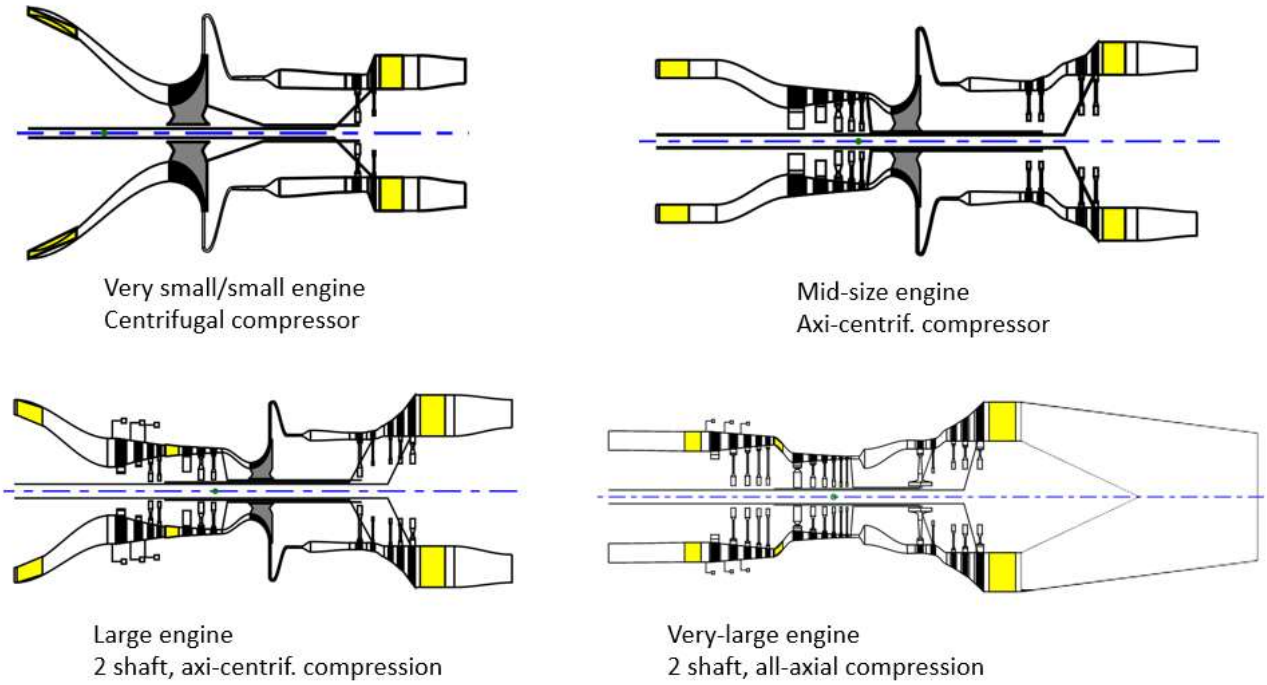

Figure 4. Representative flow path model for each power class engine (not to scale).

GAS TURBINE ENGINE OVERALL RESULTS

A summary of the engine size and performance parameters for the various engines modeled as part of this effort is located within a set of tables (Table 4, Table 5, and Table 6) in the Appendix. Engines were designed to run MRP at SLS conditions. All engine ratings assume a fixed ratio normalized by Maximum Continuous Power (MCP) as shown in Table 1. Figure 5 shows power to weight and power specific fuel consumption (PSFC) for the presented turboshaft engines. Trend lines have been added that could be useful for system studies. Advanced technology results in some impressive improvements in power-to-weight and PSFC reductions at higher power levels. For the smaller class engines, SOA and advanced engines are both already at relatively high technology levels reflected in high turbomachinery polytropic efficiencies, low core size, higher temperature materials, and better cooling. As a result of these technologies weight does not show much improvement when moving from SOA to advanced. It should be noted that the ts200a engine contains a recuperator and is not included for the curve fits due to its high weight and low PSFC. In general, a SOA is represented for a common power level then an advanced engine is developed to push this design further. The three advanced 3000 hp engines represent different visions of increasing technology, single shaft with low OPR, high OPR, and a dual shaft configuration with high OPR that incorporate design characteristics used in the T901, AATE, and T900 engines, respectively.

Table 1. Power ratings.

Rating	Description	Time limit	power
MCP	Maximum Continuous Power	continuous	100% MCP
IRP	Intermediate Rated Power	30 min.	105% MCP
MRP	Maximum Rated Power	10 min.	115% MCP
CRP	Contingency Rated Power	2.5 min.	126% MCP

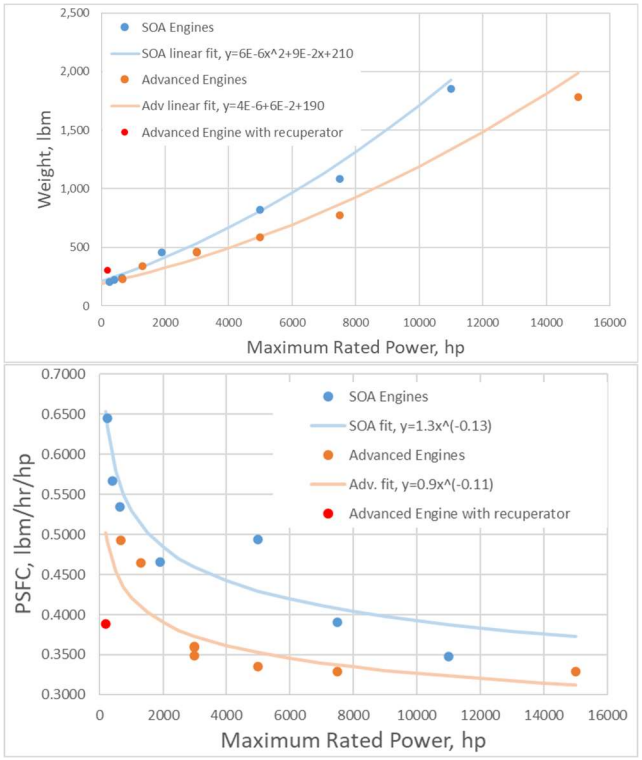

Figure 5. Engine power to weight and PSFC versus horsepower.

CFIT DISCUSSION AND RESULTS

NDARC models for these engines are generated using CFit3, a U.S. Army DEVCOM developed tool. CFit3 is a generalization of an internal curve fitting toolbox (CFit). CFit3 is written for Python 3.x.x. This software reads in real or simulated engine data and performs curve fits according to the methodology documented in the accompanying guide and is dependent on the Scipy, Numpy, and Pandas toolboxes (References 24, 25, 26). The code numerically solves for the coefficients for the RPTEM which are written into a form readable by NDARC. The RPTEM uses referred parameters to collapse and normalize engine data thereby allowing for scaling of engines for conceptual design. Of note, attempting to fit the referred parameters to engine data that is constrained by other phenomena (such as mechanical limits) results in a poor fit. Best practices are to disable these limits in the engine deck or model to collect a set of engine data, fit the referred parameters to this unconstrained dataset, reenable the limits in the source engine model, and enforce these limits outside of the RPTEM, checking to ensure consistency with the constrained dataset. RPTEM Theory is documented in the NDARC Theory Manual (Reference 6) but is summarized here for clarity. RPTEM theory was developed at the Army Aeroflight Dynamics Directorate (AFDD, now a part of DEVCOM Aviation and Missile Center) by Mike Scully and Henry Lee and first implemented by Sam Ferguson. The RPTEM assumes piecewise linear variation of engine specific power and mass flow as a function of ambient temperature ratio (θ), Mach Number and rotational speed N_r as shown below.

$$\frac{SP_a(N_{spec},\theta)}{SP_0\theta} = K_{spa}(\theta) * \left[\delta_M\sqrt{\theta_M}\right]^{X_{spa}(\theta)} \quad (1)$$

$$\frac{\dot{m}_a\ (N_{spec},\ \theta)}{\dot{m}_0 * \frac{\delta}{\sqrt{\theta}}} = e^{K_{mfa}(\theta)}\left[\delta_M\sqrt{\theta_M}\right]^{X_{xmfa}(\theta)} \quad (2)$$

θ_M and δ_M are the inlet ram temperature and pressure ratio as defined by the isentropic relations, below.

$$\theta_M = \left(1 + \frac{\gamma - 1}{2} M^2\ \right) \quad (3)$$

$$\delta_M = \left(1 + \frac{\gamma - 1}{2}\eta_d M^2\right)^{\frac{\gamma}{\gamma-1}} \quad (4)$$

η_d is the inlet recovery efficiency. CFit3 finds the piecewise linear coefficients $K_{spa}(\theta)$, $X_{spa}(\theta)$, $K_{mfa}(\theta)$, $X_{mfa}(\theta)$ and associated temperature ratio breakpoints (θ_b) to find a piecewise linear function of best fit for SP_a and $\dot{m}_a$ for a specified engine rating using a set of normalized referred engine data. Mass flow available ($\dot{m}_a$) is referred by $\frac{\delta}{\sqrt{\theta}}$ and normalized by sea level static mass flow ($\dot{m}_0$). Specific power available ($SP_a = \frac{P_a}{\dot{m}_a}$) is referred by θ and normalized by sea level static specific power (SP_0). Sample normalized referred data for static conditions are plotted in Figure 6.

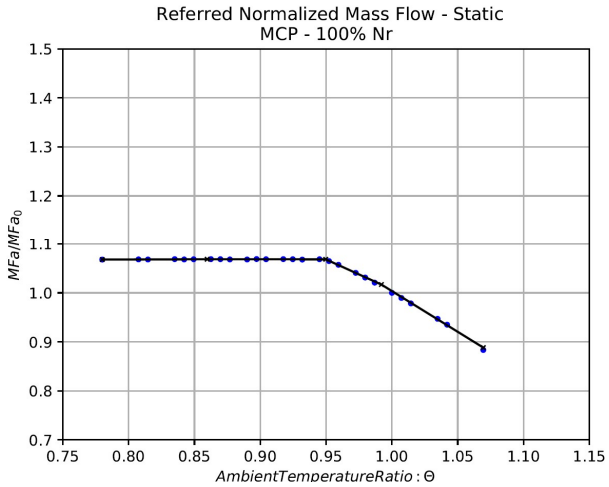

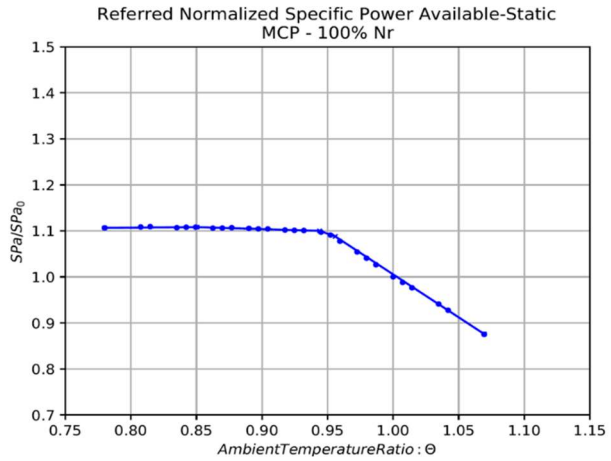

Figure 6. Reference Referred Parameter Fits

The fits are computed as follows: the piecewise linear functions Kspa(θ) and Kmfa(θ) are first determined for static conditions. The functions Xspa(θ) and Xmfa(θ) for forward flight conditions are then determined using the previously computed Kspa(θ) and Kmfa(θ). A separate function set (Kspa, Kmfa, Xspa, Xmfa) is generated for each rating code and rotational speed, N_r. These functions are evaluated by linearly interpolating in (θ,N_r) space for fixed rating code.

CFit3 computes the referred parameters and breakpoints via a combination of an optimizer (Levenberg-Marquardt) and a custom linear least squares algorithm. The optimizer chooses the interior knots p (initialized as an evenly spaced distribution on the engine data temperature ratio θ) while the minimum and maximum knots correspond to the processed engine data endpoints. From these n control points, the dataset is divided into n-1 segments where the knots are breakpoints. A linear least squares fit for the k points in a given segment is computed by

$$\begin{bmatrix} b \\ m \end{bmatrix} = \begin{bmatrix} k & \sum_{j=1}^{k} \theta_j \\ \sum_{j=1}^{k} \theta_j & \sum_{j=1}^{k} \theta_j \theta_j \end{bmatrix}^{-1} \begin{bmatrix} \sum_{j=1}^{k} y_j \\ \sum_{j=1}^{k} \theta_j y_j \end{bmatrix} \quad (5)$$

where y corresponds to either referred normalized mass flow ($\frac{\dot{m}_a}{\frac{\delta}{\sqrt{\theta}}\dot{m}_0}$) or referred normalized specific power ($\frac{SP_a}{\theta SP_0}$). At the endpoint of this line segment (a given knot p_i), the corresponding y value is computed along this least squares line as $y_i = m*p_i+b$. This process is repeated until the entire range of data is covered by these breakpoint lines. A function f_p is created that interpolates between these breakpoints. This function is evaluated across the range of θ and the (vector) error is

$$err(p) = y - f_p(\theta) \quad (6)$$

The optimizer then chooses a new set of knots p to reduce the error to near zero. Penalty functions are used to ensure that the interior knots are a reasonable distance apart (default Δθ>.01) and are bounded by the maximum and minimum θ values, preventing singularity in the matrix inversion step. Power required engine performance is based on cubic fits as a function of $q = \frac{P_q}{P_{0c}\delta\sqrt{\theta}}$, the power required normalized by referred sea level static power required at maximum continuous power (MCP), multiplied by the pressure and square root of the temperature ratio. These are multiplied by exponential functions of the temperature-Mach dependency as outlined in the NDARC theory manual. Functions for normalized referred fuel flow, mass flow, and gross thrust and are generated using SciPy's curve fit function. Fits for the ts1900s NPSS model can be seen in Figures A1-A8 in the Appendix. These fits are representative of the expected error for this tool and are similar for the other engine models developed in this paper. A flow chart of the tool chain used within this paper is shown in Figure 7.

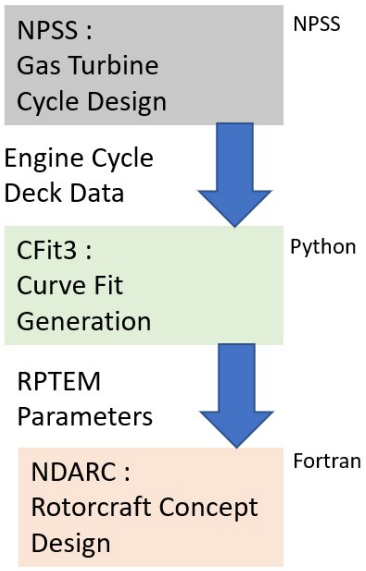

Figure 7. NPSS to NDARC flow chart.

MISSION MODELING FOR VARIOUS ENGINE TECHNOLOGY CLASSES

To illustrate the differences of advanced cycles over current cycles, a small parametric vehicle / mission analysis was performed. Public NDARC reference models for side by side, tiltwing, tandem, and large civil tiltrotor (LCTR) configurations were used for comparison and are shown in Figure 8. Background information on each is shown in References 1, 2, 27, and 28. The side by side is a six-passenger vehicle designed to operate two 37.5 nm legs or a 75 nm mission. The tiltwing can carry fifteen passengers (3,000 lbm payload), for eight 50 nm legs or 400 nm total. The tandem helicopter and LCTR are larger non-UAM concepts capable of moving 7000 lbm of useful load 88 nm and 90 passengers 1000 nm, respectively. Engine models for the NDARC models for each concept are updated based on the results in this paper. Engine mass flow, specific power, and PSFC are sized for the vehicle power requirements using a scaling method that scales up or down the baseline value using the next higher power level engine as reference. Engine weight is assumed to follow the characteristic curves shown in Figure 5. It should be clarified that the PSFC for each engine is determined with the scaling method and the curve fit shown in Figure 5 is not used for the sizing. For the side-by-side, tiltrotor, and LCTR, payload and range were maintained, and design gross weight was varied to close the design. For the tandem the load is adjusted to maintain a constant design gross weight (DGW). Each vehicle considers two or more potentially applicable engine types that are then resized with scaling to fit the concept.

Figure 8. RVLT side by side, tiltwing, tandem, and large civil tiltrotor concept vehicles (not to scale).

Table 2 and Table 3 show selected vehicle characteristics from these analyses. Results of the analysis showed that for certain engine vehicle pairs, advanced turbine engine technology achieved a 13% reduction in design gross weight, 40% reduction in engine weight, 29% reduction in fuel usage, and/or a 10% increase in useful load. The ts200a is an engine that contains a recuperator which decreases PSFC, however DGW for the vehicle increases as the technology is adopted due to the weight of the heat exchanger. Although the weight increases, the benefits in efficiency are great enough that the total vehicle fuel burn is reduced by 29%. For the non-recuperator advanced concepts, engine weight is reduced and engine efficiency is increased, which reduces fuel weight, resulting in lower vehicle DGW. Weight benefits of the advanced concepts are greater for the larger engines. The LCTR contains 4 engines and the advanced configuration results in an engine weight loss of about 40%. For the tandem helicopter the advanced configuration results in a 10% increase in useful load.

Table 2. Side by side and tiltwing resizing with different engine types.

	Side by side, 2xengines			Tiltwing, 4xengines	
Engine Type	ts200a*	ts250s	ts400s	ts650s	ts650a
Design Gross Weight, lbm	4,511	4,215	4,158	14,884	13,771
Engine power MRP, hp	337	333	321	1,164	1,082
Engine Weight, lbm	341	241	239	323	259
PSFC, hp/lbm/h	0.438	0.6313	0.598	0.5183	0.489
Fuel, lbm	155	218	206	3,566	3,199

* Includes recuperator

Table 3. LCTR and tandem helicopter resizing with different engine types.

	Large civil tiltrotor (LCTR), 4x engines		Tandem helicopter, 2xengines	
Engine Type	ts7500s	ts7500a	ts5000s	ts5000a
Design Gross Weight, lbm	119,746	103,235	30,000	30,000
Engine power MRP, hp	9,266	7,527	4,867	5,000
Engine Weight, lbm	1,559	868	790	590
PSFC, hp/lbm/h	0.3902	0.339	0.505	0.342
Fuel, lbm	17,967	12,752	6,000	6,000
Useful load for DGW, lbm			6,635	7,314

SUMMARY

Turboshaft engine performance and weight models were developed using open data sources to support conceptual propulsion and vehicle mission design and performance under the Revolutionary Vertical Lift Technology (RVLT) Project. These models range from 200 to 15,000 shaft output horsepower (150 to 11,200 kW), assuming current and advanced technology levels. Turbine engine methodology, assumptions, and resulting thermodynamic and size / weight performance are presented and trends in power specific fuel consumption and weight as a function of power are developed. These engines are translated for use in the vehicle design software, NDARC, and a description of these methods is presented. A simple propulsion performance assessment using the RVLT urban air mobility (UAM) side by side and tiltwing as well as the tandem helicopter and large civil tiltrotor reference vehicles. Advanced gas turbine engine technology can realize significant improvements in engine power-to-weight and fuel efficiency. Improved engine performance can result in significant reductions in vehicle design gross weight, engine weight and fuel usage. Engine models developed within this paper may be available upon request to primary author.

ACKNOWLEDGMENTS

The authors would like to thank the NASA Aeronautics Research Mission Directorate (ARMD), Advanced Air Vehicle Program (AAVP) / Revolutionary Vertical Lift Technology (RVLT) Project for supporting this research.

Author contact:
Jeffryes W. Chapman: jeffryes.w.chapman@nasa.gov

REFERENCES

[1] Johnson, W., Silva, C., and Solis, E., "Concept Vehicles for VTOL Air Taxi Operations," AHS Specialists' Conference on Aeromechanics Design for Transformative Vertical Flight, San Francisco, CA, 2018.

[2] Silva, C., Johnson, W., Antcliff, K. R., Patterson, M. D., "VTOL Urban Air Mobility Concept Vehicles for Technology Development," AIAA Aviation Forum, 2018 Aviation Technology, Integration, and Operations Conference, Atlanta, Georgia, USA. June 25-29, 2018.

[3] Chapman, J. W., "Multi-point Design and Optimization of a Turboshaft Engine for a Tiltwing Turboelectric VTOL Air Taxi," AIAA Scitech 2019 Forum, San Diego, California, 7-11 January 2019.

[4] Claus, R. W., Evans, A. L., Lytle, J. K., Nichols, L. D. "Numerical Propulsion System Simulation," Computing Systems in Engineering, vol. 2, no. 4, 1991, pp. 357–364.

[5] Jones, Scott M., "An Introduction to Thermodynamic Performance Analysis of Aircraft Gas Turbine Engine Cycles Using the Numerical Propulsion System Simulation Code," NASA/TM-2007-214690.

[6] Johnson, W. R., "NDARC NASA Design and Analysis of Rotorcraft," NASA/TP-2015-218751, NASA, Moffett Field, CA, 2015.

[7] Snyder, C.A. and Tong, M.T. "Modeling Turboshaft Engines for the Revolutionary Vertical Lift Technology Project." American Helicopter Society 75th Annual Forum, Philadelphia, PA, May 2019.

[8] Mattingly, J. D., *Elements of Gas Turbine Propulsion*. McGraw-Hill, Inc. New York, NY, 1996.

[9] Kerrebrock, J. L., *Aircraft Engines and Gas Turbines*, The MIT Press, Cambridge MA, 1983.

[10] Snyder, C. A., "Exploring advanced technology gas turbine engine design and performance for the Large Civil Tiltrotor (LCTR)," AIAA Propulsion and Energy Forum and Exhibition 2014, Cleveland, Ohio, USA. July 28-30, 2014.

[11] Converse, G. L.; and Giffin, R. G.: Extended Parametric Representation of Compressor, Fans and Turbines Volume I - CMGEN User's Manual. NASA Contractor Report 174645, March 1984.

[12] Gauntner, J. W., "Algorithm for Calculating Turbine Cooling Flow and the Resulting Decrease in Turbine Efficiency," NASA TM 81453, 1980.

[13] Niedzwiecki, R. W., Meitner, P. L., "Small gas turbine engine technology," NASA/Army Rotorcraft Technology. Volume 2: Materials and Structures, Propulsion and Drive Systems, Flight Dynamics and Control, and Acoustics. NASA-CP-2495-VOL-2, NAS 1.55:2495-VOL-2, Conference at Moffett Field, CA, 17-19 March 1987.

[14] Daly, M., Janes's Aero Engines 2017-2018, HIS Jane's, IHS Global Limited, Coulsdon, Surrey, UK. 2017.

[15] General Electric Aviation, "T700-701D turboshaft engines", https://www.geaviation.com/military/engines/t700-engine , https://www.geaviation.com/sites/default/files/datasheet-T700-701D.pdf , [retrieved 7, February, 2019]

[16] Kozup, Anastasia, "Army S&T Engine Demonstrator Efforts: Advanced Affordable Turbine Engine (AATE) and Future Affordable Turbine Engine (FATE)," AHS Specialists' Meeting, "Next Generation Vertical Lift Technologies, Fort Worth, Texas, February 23-25, 2011.

[17] Advanced Turbine Engine Company (ATEC), "Why two spools are better than one: Equipping our military with the best technology for existing and emerging threats", ATEC-Dual-Spool-White-Paper_2-1.pdf, https://www.atecadvantage.com/resources/white-paper/ , [retrieved 31 January, 2019]

[18] General Electric Aviation, "The Single-Spool Core: A proven design for performance and simplicity", t901-white-paper.pdf, https://www.geaviation.com/sites/default/files/t901-white-paper.pdf , [retrieved 31 January, 2019]

[19] Honeywell Aerospace, "T55 Turboshaft Engine", https://aerospace.honeywell.com/en/products/engines/t55-turboshaft-engine , n61-1492-000-000-t55turboshaftengine_bro.pdf [retrieved 5, February, 2019]

[20] General Electric Aviation, "T408-GE-400 turboshaft", https://www.geaviation.com/military/engines/t408-engine , https://www.geaviation.com/sites/default/files/brochure-t408.pdf , [retrieved 5, February, 2019]

[21] MTU Aero Engines, T64 helicopter engine, https://www.mtu.de/engines/military-aircraft-engines/helicopters/t64/ [accessed 18, March, 2019]

[22] Snyder, C. A., and Thurman, D. R., " Gas turbine characteristics for a Large Civil Tilt-Rotor (LCTR)," AHS International, 65th Annual Forum & Technology Display, Grapevine, Texas, May 27-29, 2009, NASA/TM-2010-216089.

[23] Tong, M.T., and Naylor, B.A., "An Object-Oriented Computer Code for Aircraft Engine Weight Estimation," GT2008-50062, ASME Turbo-Expo 2008, June 9-13, 2008, NASA/TM-2009-215656.

[24] Viranen, P. et. Al., "SciPy 1.0: Fundamental Algorithms for Scientific Computing in Python," *Nature Methods,* 17(3), 261-272.

[25] Harris, C.R. et. Al., "Array Programming with NumPy," Nature, 585, 357–362 (2020), DOI:10.1038/s41586-020-2649-2.

[26] McKinney, W., "Data Structures for Statistical Computing in Python," Proceedings of the 9th Python in Science Conference, Volume 445, 2010.

[27] Johnson, W., "NDARC - NASA Design and Analysis of Rotorcraft. Validation and Demonstration," AHS Aeromechanics Specialists' Conference, San Francisco, CA, January 20-22, 2010.

[28] Acree, C.W., Jr. "Integration of Rotor Aerodynamic Optimization with the Conceptual Design of a Large Civil Tiltrotor." American Helicopter Society Specialists' Conference on Aeromechanics, San Francisco, CA, January 2010.

APPENDIX

Table 4. Very Small/Small engine size and performance parameters.

Engine name	ts200a	ts250s	ts400s	ts650s	ts650a
Maximum rated hp/kw, Sea level, ISA	200/ 150	250/ 186	400/ 300	650/ 485	660/ 492
Technology	Advanced	Current	Current	Current	Advanced
Power specific fuel consumption, PSFC, lb/hr/hp	0.3887	0.6449	0.5672	0.5341	0.4926
Airflow, lb/s	2	2	3	5	4
OPR	5	6	8	9	9
Compressor stage layout (A=axial, C=centrifugal)	1C	1C	1C	1C	1C
Turbine stages	1 + 1	2 + 2	1 + 1	1 + 1	1 + 1
Diameter in	12	12	12	16	16
Length, in	29	26	31	28	28
Weight, lb	305*	205	222	242	231
Power/weight, hp/lb	0.66*	1.22	1.80	2.69	2.86

* Includes recuperator

Table 5. Mid-engine size and performance parameters.

Engine name	ts1300a	ts1900s	ts3000a1_25	ts3000a1_18	ts3000a2
Maximum rated hp/kw, Sea level, ISA	1,300/ 970	1,895/ 1,413	3,000/ 2,237	3,000/ 2,237	3,000/ 2,237
Technology	Advanced	Current	Advanced	Advanced	Advanced
Power specific fuel consumption, PSFC, lb/hr/hp	0.4650	0.4661	0.3601	0.3598	0.3484
Airflow, lb/s	9	12	15	12	14
OPR	14	18	25	18	25
Compressor stage layout (A=axial, C=centrifugal)	2C	5A / 1C	6A / 1C	5A / 1C	4A+ 3A / 1C
Turbine stages	2 + 2	2 + 2	2 + 3	2 + 4	1 + 1 + 3
Diameter in	20	20	16	16	17
Length, in	34	45	47	47	48
Weight, lb	342	459	458	460	455
Power/weight, hp/lb	3.8	4.14	6.55	6.52	6.59

Table 6. Large/Very Large engine size and performance parameters.

Engine name	ts5000s	ts5000a	ts7500s	ts7500a	ts11000s	ts15000a
Maximum rated hp/kW, Sea level, ISA	5,000/ 3,730	5,000/ 3,730	7,248/ 5,400	7,500/ 5,593	11,000/ 8,203	15,000/ 11,185
Technology	Current	Advanced	Mid	Advanced	Current	Advanced
Power specific fuel consumption, PSFC, lb/hr/hp	0.4942	0.3358	0.3909	0.3293	0.3481	0.3295
Airflow, lb/s	28	20	36	28	55	50
OPR	9	28	20	30	25	25
Compressor stage layout (A=axial, C=centrifugal)	7A / 1C	4A + 3A / 1C	5A / 1C	4A + 3A / 1C	5A + 6A	5A + 7A
Turbine stages	2 + 2	1 + 1 + 3	2 + 3	1 + 1 + 3	1 + 1 + 3	1 + 1 + 3
Diameter in	24	20	27	25	33.7	36.3
Length, in	48.8	53	58	59	115.7	120.5
Weight, lb	823	584	1085	773	1,852	1,784
Power/weight, hp/lb	5.94	8.56	6.91	9.70	5.94	8.41

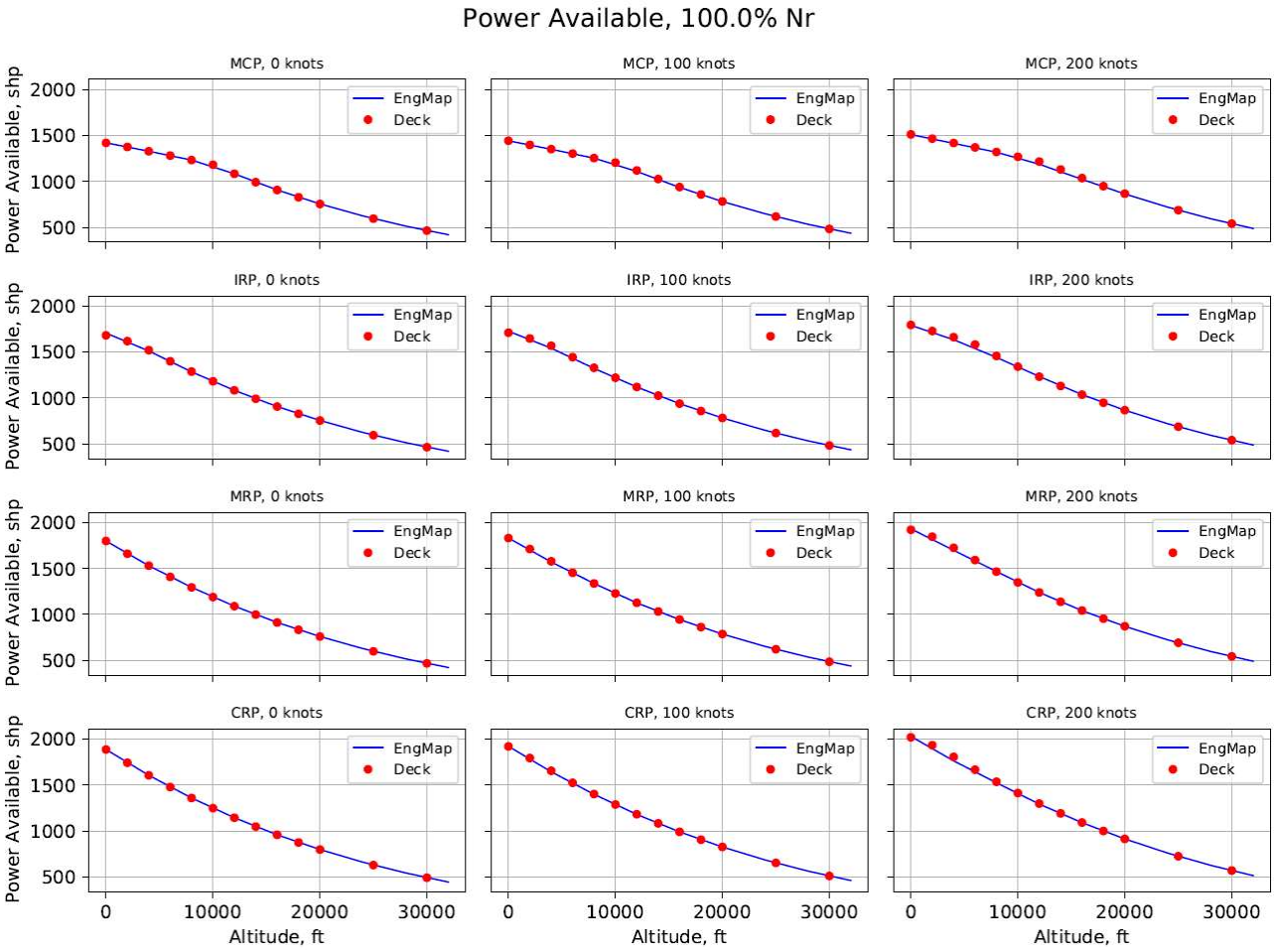

Figure A1: Sample CFit3 Power Available Fits (100%Nr)

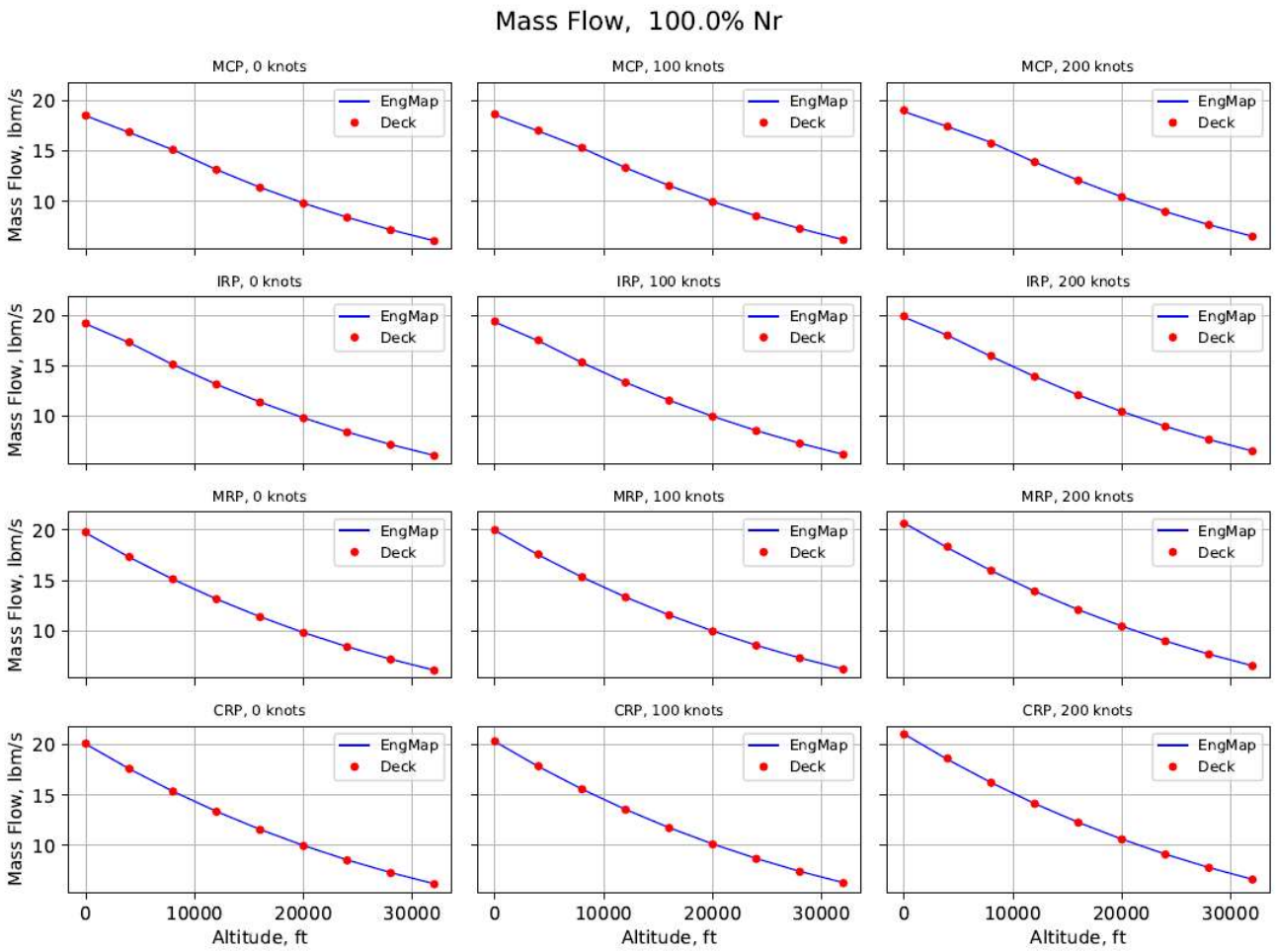

Figure A2: Sample Mass Flow Fits (100%Nr)

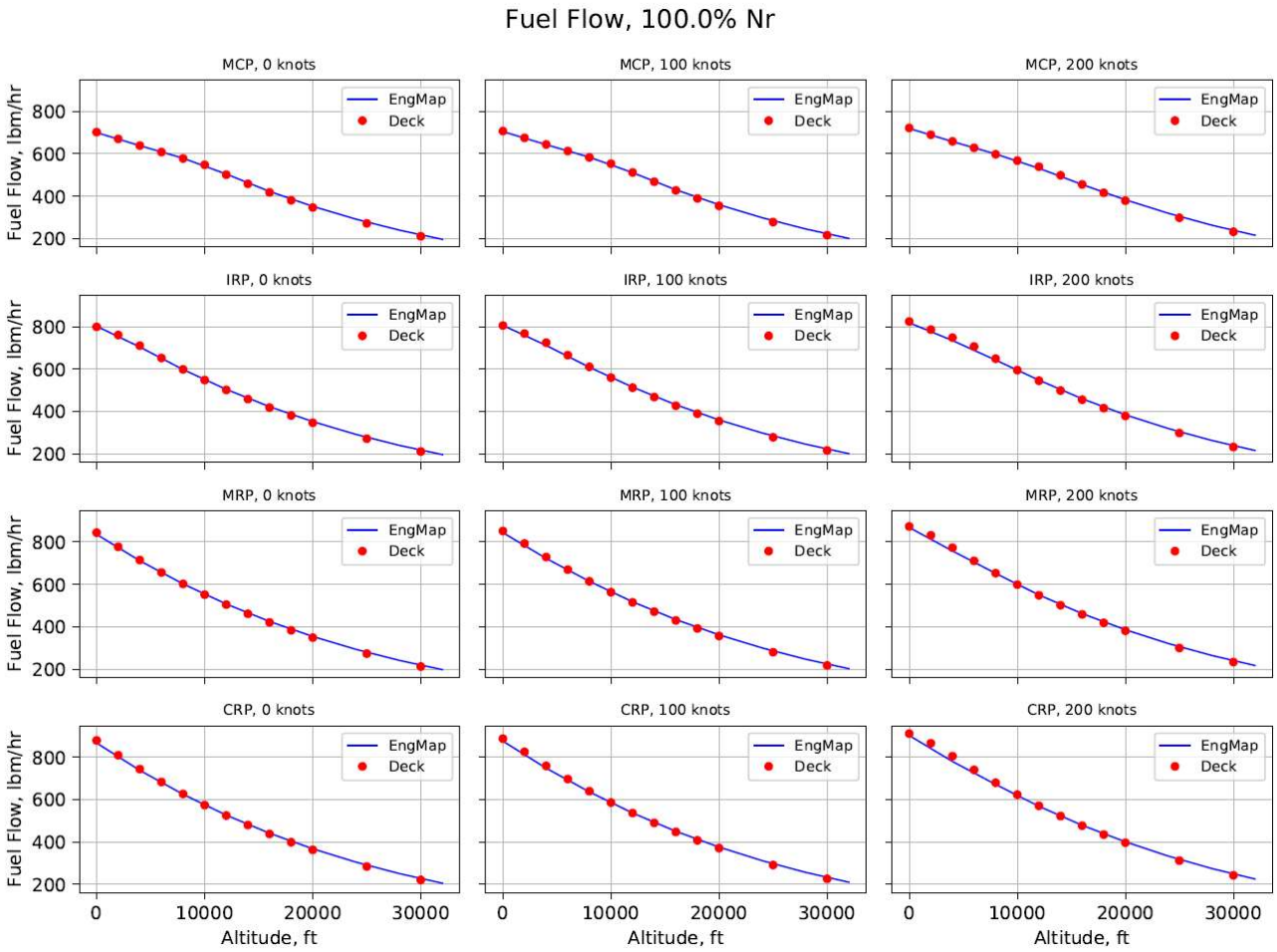

Figure A3: Sample CFit3 Fuel Flow Available Fits (100%Nr)

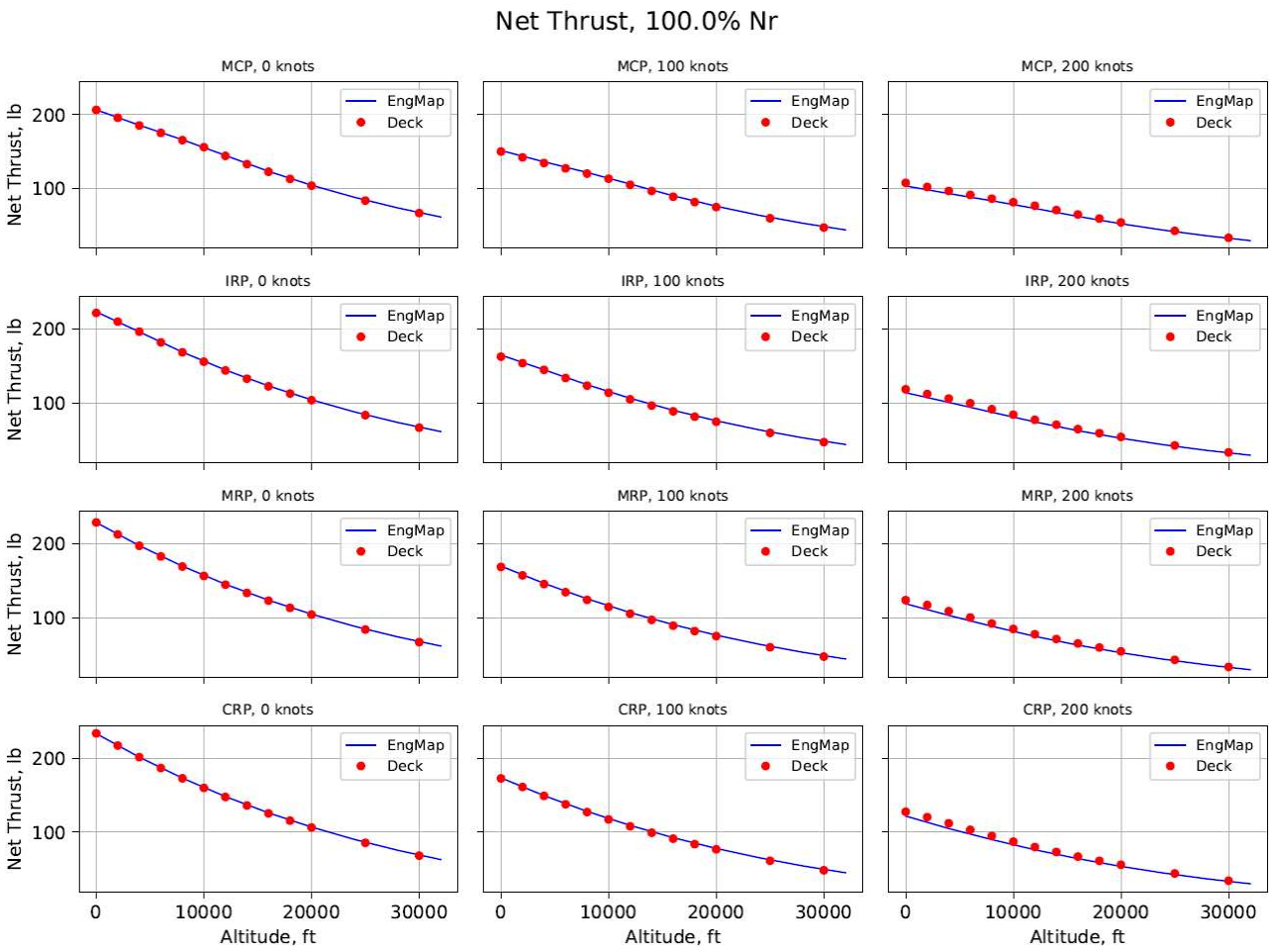

Figure A4: Sample CFit3 Net Thrust Fits (100%Nr)

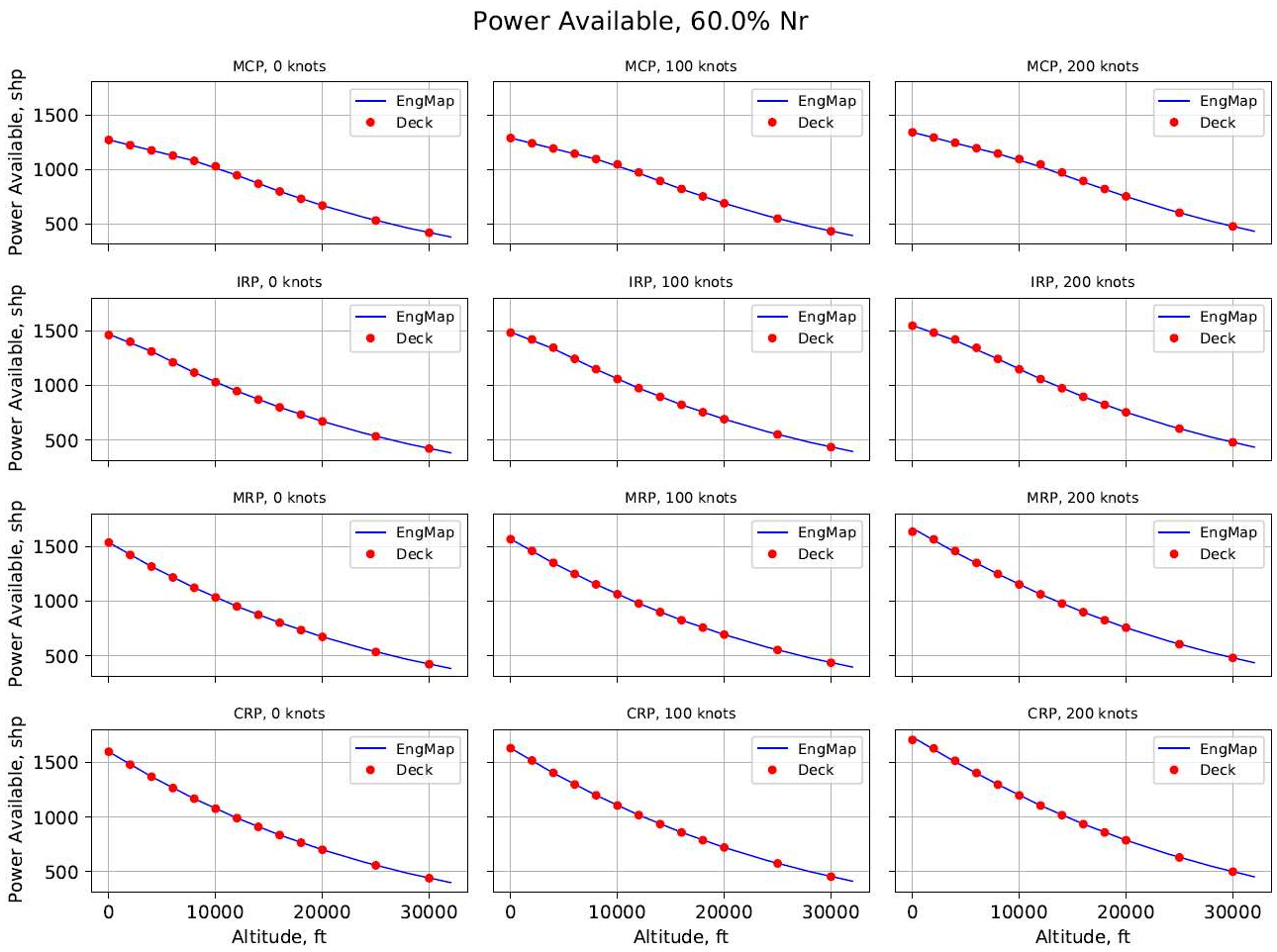

Figure A5: Sample CFit3 Power Available Fits (60%Nr)

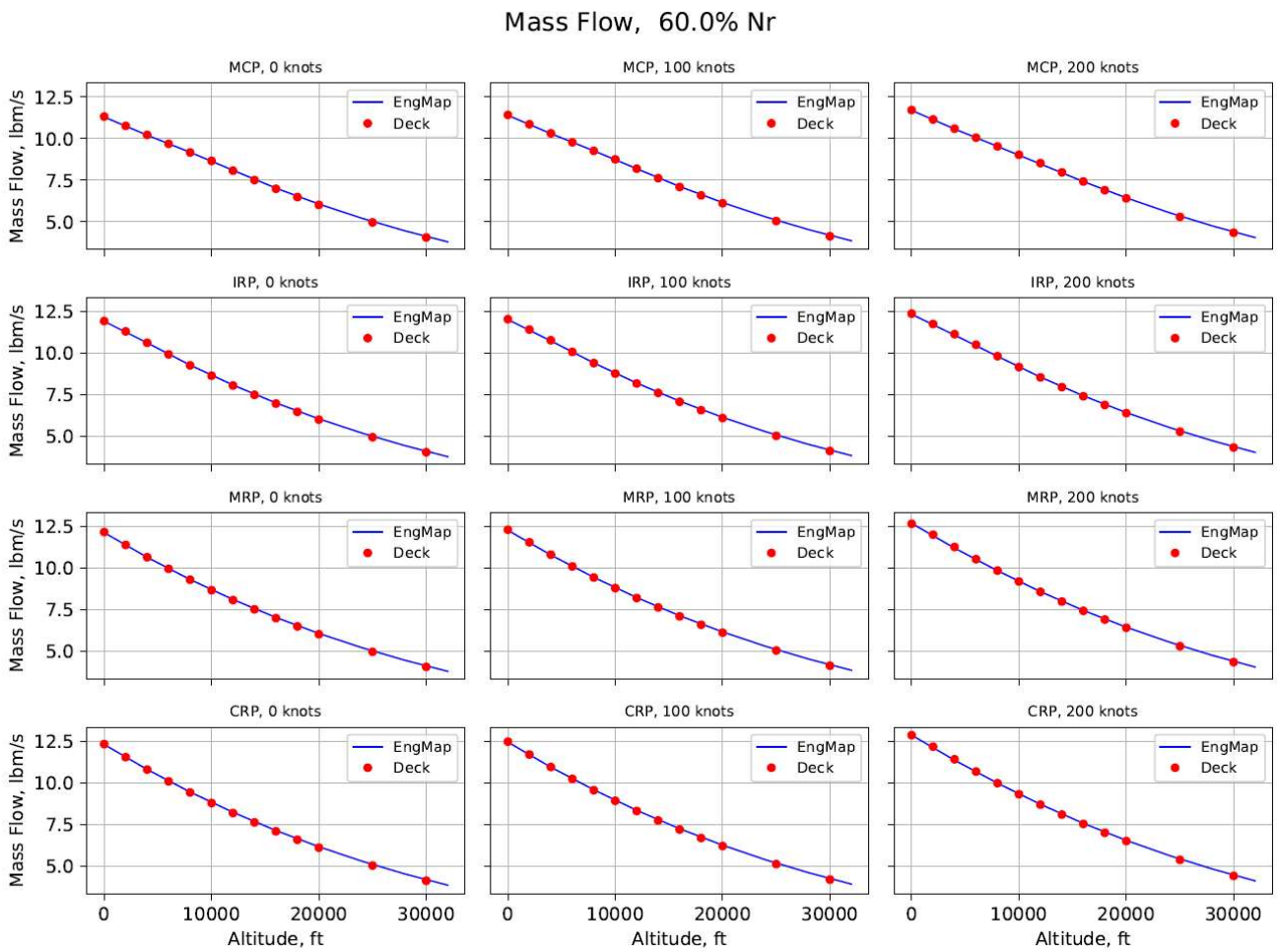

Figure A6: Sample CFit3 Mass Flow Fits (60%Nr)

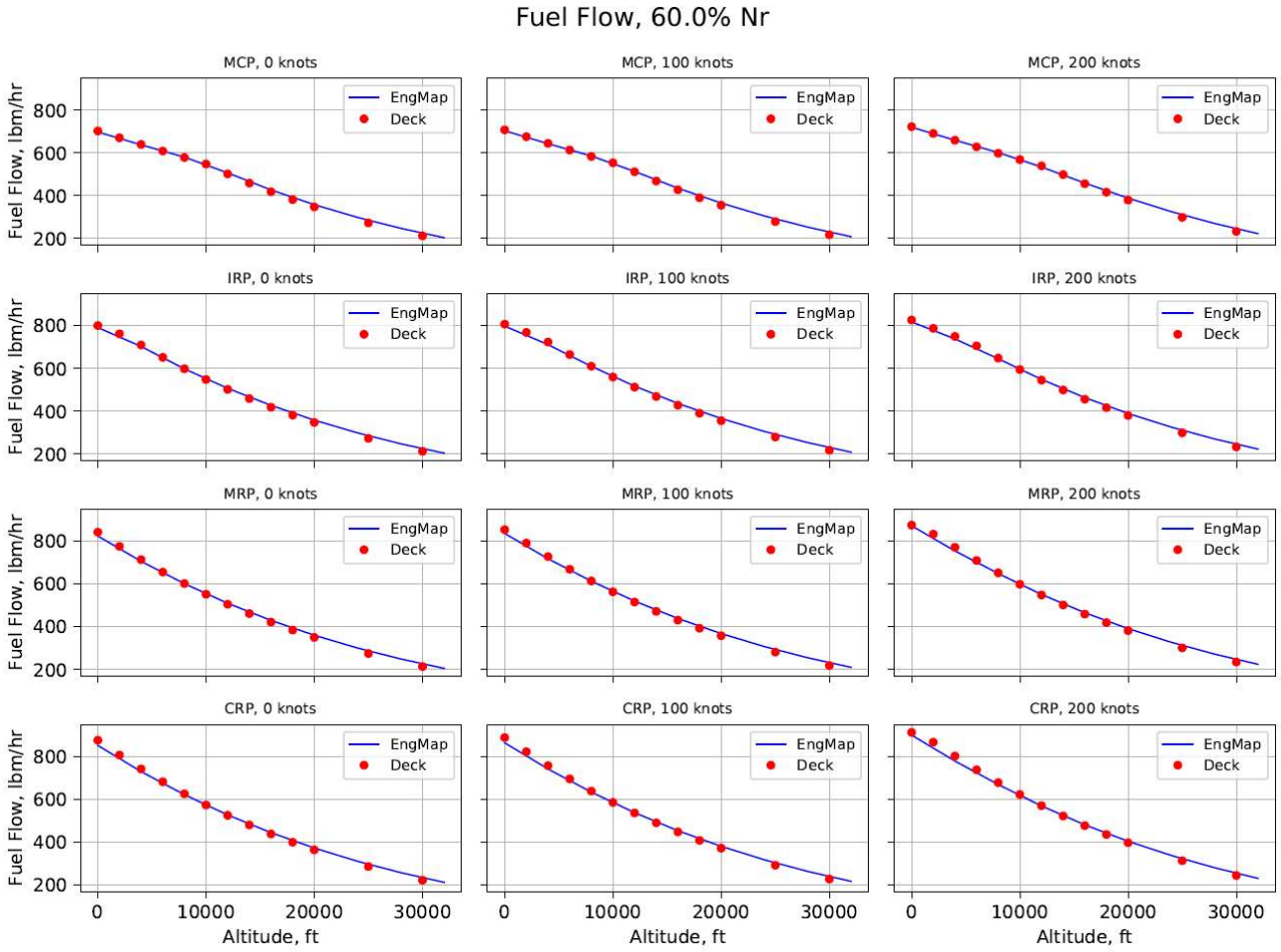

Figure A7: Sample CFit3 Fuel Flow Fit (60%Nr)

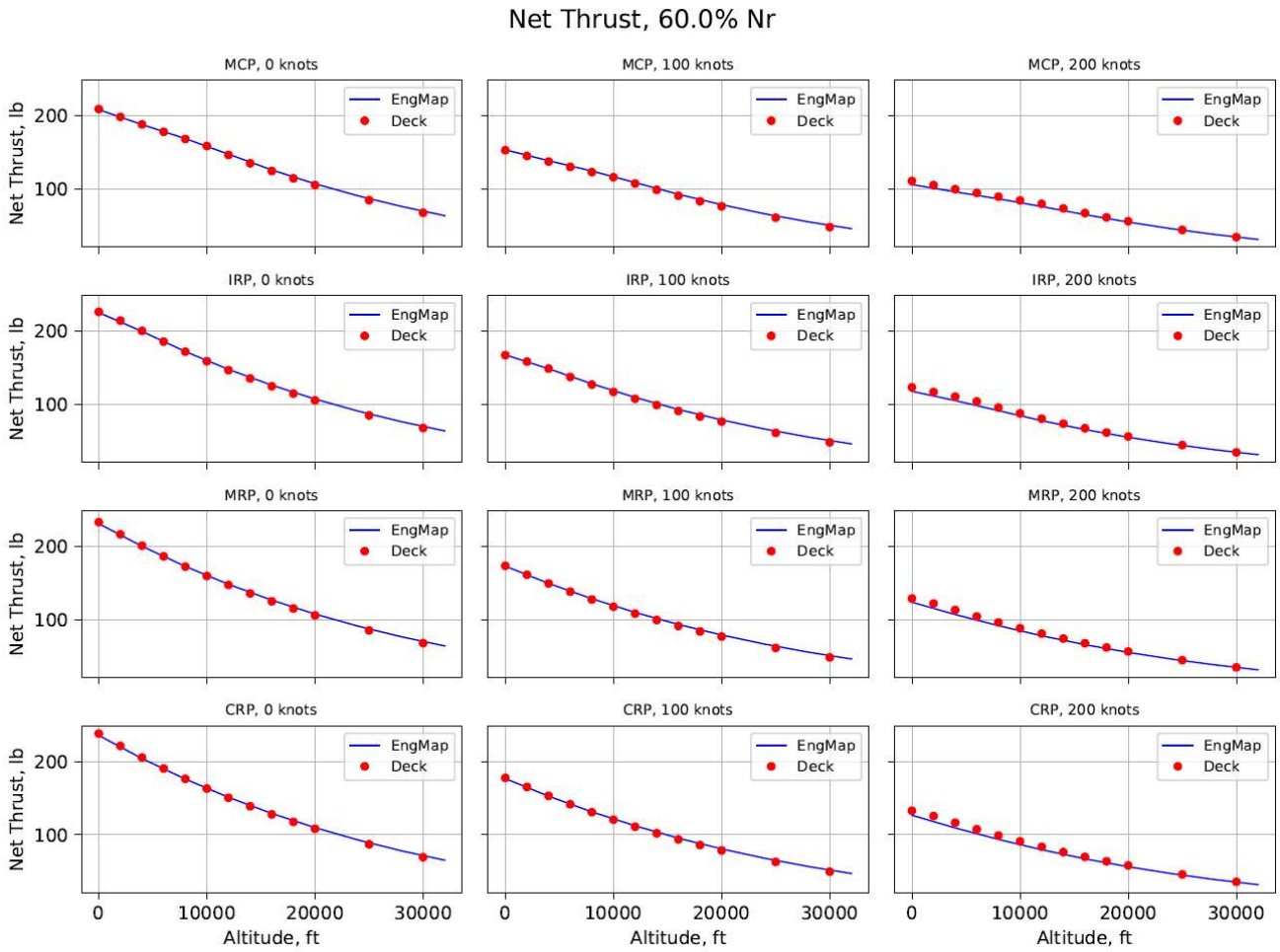

Figure A8: Sample CFit3 Net Thrust Fits (60%Nr)